J. Chem. Eng. Data **2007,** *52,* 1975−1978 **1975**

Fusion Curves and Enthalpy and Internal Energy Changes of Benzene, Nitrobenzene, Bromobenzene, and Chlorobenzene at Pressures up to 3500 MPa

Wei Xu,[†] Rongjiao Zhu,[†] Yiling Tian,*[,†] Hongling Li,[‡] and Hesong Li[†]

Department of Chemistry, Institute of Science, Tianjin University, Tianjin 300072, People's Republic of China, and Institute of Chemical Engineering, Shihezi University, Shihezi 832003, People's Republic of China

The fusion temperature as a function of pressure for benzene, nitrobenzene, bromobenzene, and chlorobenzene at pressures up to 3500 MPa has been determined. The new experimental data are an extension to higher pressures and temperatures of previous data and fitted by the equation $T_{\mathrm{fus}} = T_0(1 + \Delta p/a_1)^{a_2} \exp(-a_3\Delta p)$. Changes of the molar enthalpy and the molar internal energy on fusion were calculated using the parameters of the fitted equation. Comparisons with data from references show that the experimental data, parameters of fitted equations, molar enthalpy changes, and molar internal energy changes are reliable.

Introduction

Some substances show unusual physical properties at high pressure; therefore, studies on the properties of these substances at high pressure are attracting increasing interest. Theoretical calculation indicates that, at sufficiently high pressure, all matter is converted to a metallic form. This has been verified for I_2 and C_SI.[1]

Fusion transition can be useful for the calibration of pressure devices because the transition is quite sharp (small hysteresis) and can be detected easily by using either direct or indirect methods. Methods used to detect phase transition include measurement of electrical resistance, volume, refractive index, absorption reflectance, X-ray diffraction, neutron diffraction differential thermal analysis, magnetic properties, and capacitance. Bridgman[2−4] investigated the fusion curves of a number of organic substances up to 1200 MPa. Osugi et al.[5] determined the high-pressure liquid−solid transitions of benzene, chlorobenzene, and toluene at 298 K. Crawford[6] studied the melting curves of Kr, Ne, and He. Strong[7] researched iron and gold. Akella[8] presented melting points of copper, gold, and silver.

This paper describes the experimental method that was developed to determine fusion temperatures and pressures of benzene, nitrobenzene, bromobenzene, and chlorobenzene between (246 and 663) K at pressures up to 3500 MPa. Equations for the pressure dependence of the fusion temperature based on thermodynamic principles were obtained. Changes of the molar enthalpy and molar internal energy *s* on fusion were calculated using the parameters of fitted equations and the molar volume changes.

Theoretical Models

Fusion is considered as an ordinary first-order phase transition (the two-phase approach to fusion). In accordance with the thermodynamic theory, the fusion occurs when the Gibbs free energies of the liquid and solid are equal at a given temperature and pressure. The thermodynamic relationship for liquid−solid equilibrium is given by Clapeyron equation[9]

$$\frac{\mathrm{d}\ln T_{\mathrm{fus}}}{\mathrm{d}p_{\mathrm{fus}}} = \frac{\Delta_{\mathrm{fus}}V}{\Delta_{\mathrm{fus}}H} \tag{1}$$

where T_{fus} is the absolute fusion temperature and $\Delta_{\mathrm{fus}}H = T_{\mathrm{fus}}\Delta_{\mathrm{fus}}S$ is the fusion enthalpy; $\Delta_{\mathrm{fus}}S$ is the entropy change during fusion. $\Delta_{\mathrm{fus}}V = V_{\mathrm{liq}} - V_{\mathrm{sol}}$ is the volume change on fusion. If $\Delta_{\mathrm{fus}}V > 0$, the fusion temperature increases with pressure; if $\Delta_{\mathrm{fus}}V < 0$, it decreases; and if $\Delta_{\mathrm{fus}}V = 0$, the fusion curve has its maximum.[10] This approach can be used in thermodynamic calculation through different approximations of the equation of state for the solid and liquid phases.[11,12]

Equation 1 can be written as a fractional form function by performing Padé $[L/M]$ approximation

$$\frac{\mathrm{d}\ln T_{\mathrm{fus}}}{\mathrm{d}p} = \frac{c_0 + c_1\Delta p + ... + c_L(\Delta p)^L}{b_0 + b_1\Delta p + ... + b_M(\Delta p)^M} \tag{2}$$

where $\Delta p = p - p_0$, p_0 is some reference (for example, triple point) pressure. $c_0, c_1, ..., c_L$ and $b_0, b_1, ..., b_M$ are constants. Equation 2 combines both one-phase and two-phase approaches to fusion. The integration of eq 2 with respect to pressure leads to the fusion curve equation $T_{\mathrm{fus}} = F_{[L/M]}(x)$.

For $M = 1$

$$T_{\mathrm{fus}} = F_{[L/1]}(x) = F_{[0/1]}(x) \exp\left(-\sum_{k=1}^{L} a_{k+2}x^k\right) = T_0(1 + x)^{a_2} \exp\left(-\sum_{k=1}^{L} a_{k+2}x^k\right) \tag{3}$$

For $M = 2$

$$T_{\mathrm{fus}} = F_{[L/2]}(x) = F_{1/2}(x) \exp\left(-\sum_{k=2}^{L} a_{k+3}x^{k-1}\right) = T_0(1 + x)^{a_2}(1 + a_3x)^{-a_4} \exp\left(-\sum_{k=2}^{L} a_{k+3}x^{k-1}\right) \tag{4}$$

---

* Corresponding author. Telephone: +86-22 27406140. Fax: +86-22 27403475. E-mail: yltian@tju.edu.cn.

[†] Tianjin University.

[‡] Shihezi University.

10.1021/je700276z CCC: $37.00

Here $x = \Delta p/a_1$ is the reduced pressure, a_1 has the dimensionality of pressure, and the other parameters are dimensionless. The parameters a_k in eqs 3 and 4 can be expressed in terms of c_k and b_k.

Fusion curves have universal features irrespective of whether they rise or fall, are smooth, and are concave toward pressure. It follows from these conditions that the parameters a_k in eqs 3 and 4 are positive.

For eqs 3 and 4, the fusion equations have the same structure

$$T_{\text{fus}} = F_{[0/1]}(x)D_{\text{fus}}(x) \tag{5}$$

where $F_{[0/1]}(x)$ is the rising and $D_{\text{fus}}(x)$ the damping function that asymptotically slopes down under pressure. The function $F_{[0/1]}(x)$ is the Simon−Glatzel empirical equation for fusion, which can be written in the form[13]

$$T_{\text{fus}} = T_0(1 + \Delta p/a)^{1/c} \tag{6}$$

where T_0 is the temperature at triple point and $\Delta p = p - p_0$. $D_{\text{fus}}(x)$ is usually expressed by $\exp(-a_3\Delta p)$ in this paper.

Expanding eq 2 at point $\Delta p = p - p_0$ up to the second order, one obtains

$$\frac{\mathrm{d}\ln T_{\text{fus}}}{\mathrm{d}p} = y \approx y_0 + y_0'\,\Delta p + \frac{1}{2}y_0''\,(\Delta p)^2 \tag{7}$$

where single and double primes denote the first- and second-order derivatives, respectively, with respect to pressure. Performing the Padé approximation to the right side, we obtain

$$\frac{\mathrm{d}\ln T_{\text{fus}}}{\mathrm{d}p} = \frac{1 - \beta\Delta p}{\sigma(\alpha + \Delta p)} \tag{8}$$

where the parameters α, β, and σ are given by $\alpha = -y_0'/y_0''$, $\beta = y_0''/2y_0' - y_0'/y_0$, and $\sigma = -y_0''/2y_0y_0'$.

By integrating eq 8 wth respect to pressure, one obtains the equation for pressure dependence of fusion temperature in the form

$$T_{\text{fus}} = T_0(1 + \Delta p/a_1)^{a_2}\exp(-a_3\Delta p) \tag{9}$$

where $a_1 = \alpha$, $a_2 = (1 + \alpha\beta)/\sigma = y_0'\alpha^2$, and $a_3 = \beta/\sigma = -y_0'\alpha - y_0$.

Note that the fusion curve can be predicted if the constants in eq 9 at the reference pressure are known.

Experiment Section

Materials and Their Purities. Because impurities lower the fusion temperature of a solvent, all reagents were purified. Benzene, nitrobenzene, bromobenzene, and chlorobenzene were fractionally recrystallized five times. A mass spectroscopic analysis of all reagents showed that purities were all above 99.99 mass %. The samples used were degassed for 4 h at temperatures of (1 to 2) K below their respective normal fusion temperatures.

Experimental Apparatus and Accuracy. The experiments were performed in a high-pressure autoclave with a movable piston, which has been described previously.[14] The tube-like autoclave is made of austentitic manganese steel and has a length of 300 mm and outer and inner diameters of 120 mm and 20 mm, respectively. The piston body is modified for high pressure, and the piston operates using a three-order multiplying pressure function. After samples were introduced into the autoclave, the temperatures were changed while maintaining a constant pressure, which could be achieved by adjusting the movable piston. Temperatures were decreased stepwise at a rate of 2 K·h^{-1} until the estimated freezing temperature was reached.

The system pressures were measured with a strain gauge dilating-cylinder pressure transducer. A detailed description has been reported by Jäger and Wanninger.[15] For this device, the ratio of the external and internal diameters of the cylinder, κ, is equal to 5.0. The output, $I(p)$, from the gauge for either rising or falling pressures showed a reproducibility of 0.03 % of full scale. The estimated maximum uncertainty for high pressure was about ±2.0 MPa. To achieve isothermal conditions for this dilating cylinder, a water jacket (at 273 K) was used to stabilize the casing temperature and great care was exercised to avoid pressure-induced temperature change in the pressure-transmitting fluid. The I, p curve was calibrated using the mercury melting point curve. The maximum deviation of pressure from linearity was 2.67 MPa due to hysteresis effect. The temperatures of the vessel were measured with a platinum resistance thermometer with an estimated maximum uncertainty of ±0.02 K.

Experimental Procedure. One way to experimentally determine a solid−liquid equilibrium temperature (fusion temperature) at constant pressure is to use thermal analysis. The experiments were performed as sample cooling experiments. The temperature of a system will remain constant at the freezing temperature, although a slight dip below the freezing temperature can occur due to supercooling. To reduce the supercooling effect, nanometer-sized SiO_2 was added to the samples in any experiment. Prior to the introduction of the sample into the autoclave, the equipment was dried, evacuated, and flushed with pure sample. For temperatures below 173 K, the cooling medium in the autoclave jacket was liquid nitrogen. In the range of (173 to 273) K, the cooling medium was ethanol cooled by a mixture of liquid nitrogen and dry ice. When the temperatures were in the range of (273 to 353) K, water was used. For temperatures greater than 353 K, anhydrous glycerin was used.

During the cooling process, the volume decreased; therefore, a movable piston was used to keep the pressure constant. The above procedure was repeated at other pressures to obtain the p, T fusion curves.

Results and Discussion

Most substances freeze at a higher temperature when subject to pressure. It is as though the pressure is preventing the formation of the solid phase from the less dense liquid phase. Exceptions to this behavior include water, for which the liquid is denser than the solid. We can rationalize the response of fusion temperatures to pressures as follows. The variation of the chemical potential with pressure is expressed by

$$\left(\frac{\partial\mu}{\partial p}\right)_T = V_{\text{m}} \tag{10}$$

This equation shows that the slope of chemical potential against pressure is equal to the molar volume of the substance. An increase in pressure raises the chemical potential of any pure substance (because $V_{\text{m}} > 0$). In most cases, $V_{\text{m}}(\text{l}) > V_{\text{m}}(\text{s})$, and the equation predicts that an increase in pressure increases the chemical potential of the liquid more than that of the solid. The effect of pressure in such a case is to raise the fusion temperature slightly.

Table 1 gives the fusion temperatures T_{fus}, changes of molar volume $\Delta_{\text{fus}}V_{\text{m}}$ from refs 3 and 4, changes of molar enthalpy $\Delta_{\text{fus}}H_{\text{m}}$, and changes of molar internal energy $\Delta_{\text{fus}}U_{\text{m}}$ on fusion at pressures up to 3500 MPa for benzene, nitrobenzene, bromobenzene, and chlorobenzene. As the pressure increases, the unoccupied space left by the uncoordinated motion of the

Table 1. Fusion Temperatures T_{fus}, Molar Volume Changes $\Delta_{\mathrm{fus}}V_{\mathrm{m}}$ from References 3 and 4, Molar Enthalpy Changes $\Delta_{\mathrm{fus}}H_{\mathrm{m}}$, and Molar Internal Energy Changes $\Delta_{\mathrm{fus}}U_{\mathrm{m}}$ on Fusion for Benzene, Nitrobenzene, Bromobenzene, and Chlorobenzene

	benzene				nitrobenzene			
p/MPa	T_{fus}/K	$\Delta_{\mathrm{fus}}V_{\mathrm{m}}$/cm^3·mol^{-1}	$\Delta_{\mathrm{fus}}H_{\mathrm{m}}$/kJ·mol^{-1}	$\Delta_{\mathrm{fus}}U_{\mathrm{m}}$/kJ·mol^{-1}	T_{fus}/K	$\Delta_{\mathrm{fus}}V_{\mathrm{m}}$/cm^3·mol^{-1}	$\Delta_{\mathrm{fus}}H_{\mathrm{m}}$/kJ·mol^{-1}	$\Delta_{\mathrm{fus}}U_{\mathrm{m}}$/kJ·mol^{-1}
100	306.44	8.0145	9.95	9.15	299.74	9.0190	12.50	11.60
200	329.93	6.8115	9.93	8.56	320.77	8.1733	12.71	11.08
300	351.25	5.9289	9.94	8.16	340.02	7.4506	12.92	10.69
400	370.85	5.2727	10.02	7.91	360.41	6.8351	13.25	10.52
500	389.07	4.7962	10.21	7.81	378.61	6.3672	13.63	10.44
600	406.15	4.4056	10.40	7.75	395.9	6.0139	14.05	10.45
700	422.25	4.0776	10.59	7.74	412.3	5.7135	14.44	10.44
800	437.52	3.7885	10.76	7.73	427.24	5.4353	14.84	10.49
900	452.06	3.5229	10.87	7.70	442.98			
1000	465.96	3.2964	11.00	7.71	462.61			
1500	538.73				516.38			
2000	584.85				565.62			
2500	625.73				595.88			
3000	663.67				614.38			

	bromobenzene				chlorobenzene			
p/MPa	T_{fus}/K	$\Delta_{\mathrm{fus}}V_{\mathrm{m}}$/cm^3·mol^{-1}	$\Delta_{\mathrm{fus}}H_{\mathrm{m}}$/kJ·mol^{-1}	$\Delta_{\mathrm{fus}}U_{\mathrm{m}}$/kJ·mol^{-1}	T_{fus}/K	$\Delta_{\mathrm{fus}}V_{\mathrm{m}}$/cm^3·mol^{-1}	$\Delta_{\mathrm{fus}}H_{\mathrm{m}}$/kJ·mol^{-1}	$\Delta_{\mathrm{fus}}U_{\mathrm{m}}$/kJ·mol^{-1}
100	259.05	7.6307	10.82	10.06	246.40			
200	276.45	6.7200	11.26	9.92	263.03	6.3596	10.68	9.40
300	292.45	5.9978	11.57	9.78	273.46	5.7518	11.03	9.30
400	310.05	5.4168	11.81	9.64	288.44	5.2791	11.39	9.27
500	322.55	4.9458	12.00	9.53	301.03	4.8626	11.66	9.23
600	336.15	4.5219	12.07	9.35	315.62	4.5024	11.89	9.19
700	349.25	4.1765	12.14	9.22	325.56	4.1872	12.09	9.15
800	361.85	3.8938	12.24	9.12	336.87	3.9283	12.31	9.16
900	374.75	3.6740	12.40	9.09	348.81	3.6920	12.48	9.16
1000	382.85	3.4856	12.56	9.07	354.76	3.5006	12.71	9.21
1500	430.05				403.44			
2000	473.67				440.81			
2500	514.22				473.28			
3000	553.94				503.63			
3500	587.21				530.87			

molecules of the liquid would be expected to become smaller, so that $\Delta_{\mathrm{fus}}V_{\mathrm{m}}$ would become less. $\Delta_{\mathrm{fus}}H_{\mathrm{m}}$ computed from Clapeyron's equation increases slightly with increasing pressure. $\Delta_{\mathrm{fus}}U_{\mathrm{m}}$ differs from the change of $\Delta_{\mathrm{fus}}H_{\mathrm{m}}$ only by the external work $p\Delta_{\mathrm{fus}}V_{\mathrm{m}}$. $\Delta_{\mathrm{fus}}U_{\mathrm{m}}$ slightly decreases and would be constant at high pressures. For benzene $\Delta_{\mathrm{fus}}U_{\mathrm{m}}$ is close to 7.70 kJ·mol^{-1}, that for nitrobenzene is 10.44 kJ·mol^{-1}, that for bromobenzene is 9.07 kJ·mol^{-1}, and that for chlorobenzene is 9.15 kJ·mol^{-1}. This phenomenon relates to the intrinsic shapes of the molecules limiting the motion of the molecules at high pressures.

Figure 1 presents experimental points of this work, previously published results, and the least-squares fitting fusion curves using eq 9 for benzene, nitrobenzene, bromobenzene, and chlorobenzene. Changing trends of four curves are consistent with conclusions of the above thermodynamic relations of eq 10. The equation provides good description for the experimental results. The fractional deviations of the experimental fusion temperatures from calculated values are illustrated in Figure 2. These deviations are less than 1.0 % except for one point. For benzene, Tammann[16] predicted that the maximum of the fusion curve would be about 700 MPa but that there would be no explicit temperature of the maximum point. Both Bridgman's results up to 1200 MPa and our experimental results up to 3000 MPa showed no maximum. For nitrobenzene, Tammann[16] assumed a maximum fusion point at 1000 MPa and 397 K;

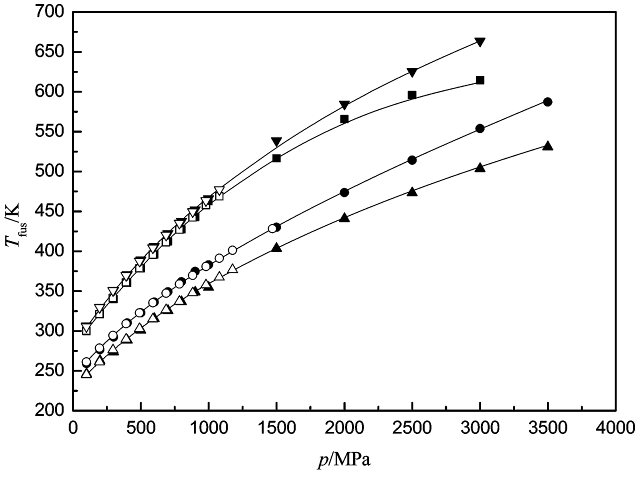

Figure 1. Fusion curves of benzene (▼, this work; ▽, ref 3), nitrobenzene (■, this work; □, ref 3), bromobenzene (●, this work; ○, ref 4), and chlorobenzene (▲, this work; △, ref 4). Lines are the fitted curves.

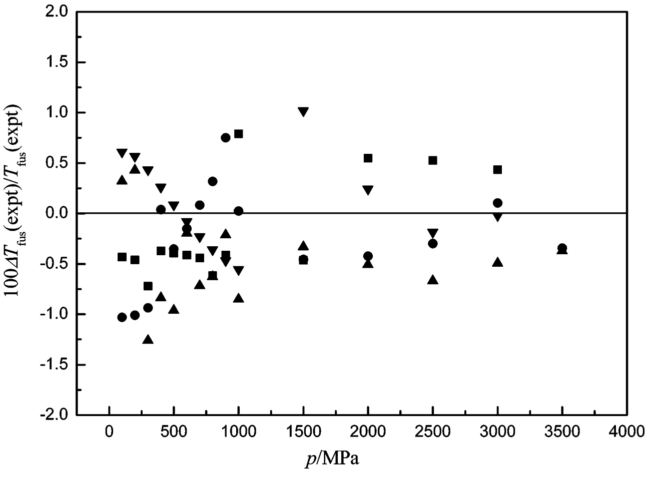

Figure 2. Fractional deviations $\Delta T_{\mathrm{fus}}(\mathrm{exptl}) = T_{\mathrm{fus}}(\mathrm{exptl}) - T_{\mathrm{fus}}(\mathrm{calcd})$ of the experimental fusion temperatures $T_{\mathrm{fus}}(\mathrm{exptl})$ from calculated values $T_{\mathrm{fus}}(\mathrm{calcd})$: ▼, benzene; ■, nitrobenzene; ▲, chlorobenzene; ●, bromobenzene.

Table 2. Least-Squares Fitting Parameters Used in Equation 9

substance	T_0/K[17]	a_1/GPa	a_2	a_3/GPa	δ/K[a]
benzene	278.82	0.5156	0.5245	0.0465	1.67
nitrobenzene	278.80	0.9793	1.0008	0.2058	2.22
bromobenzene	242.10	0.4231	0.3536	0.0291	1.49
chlorobenzene	227.70	0.5237	0.4414	0.0143	2.17

[a] Average deviation: $\delta = \overline{|T_{\mathrm{fus}}(\mathrm{exptl}) - T_{\mathrm{fus}}(\mathrm{calcd})|}$.

however, neither Bridgman nor our experiments obtained this supposed maximum. For bromobenzene and chlorobenzene, there was still no maximum of the fusion curves in either the studies of Bridgman or our experiments.

Table 2 lists the parameters T_0, a_1, a_2, and a_3 in eq 9 obtained using a nonlinear least-squares fitting procedure. The average deviations between measured and calculated values are also given in this table. For substances discussed here, p_0 is rather smaller than p and, hence, p_0 would be neglected. In all cases the fitting results are as good as the experimental data.

Figures 3 and 4 show the deviations of the calculated changes of molar enthalpy and the molar internal energy on fusion from those values of refs 3 and 4, respectively. For benzene, nitrobenzene, bromobenzene, and chlorobenzene, the deviations are almost less than 0.3 kJ·mol^{-1}, which means that these calculated $\Delta_{\mathrm{fus}}H_{\mathrm{m}}$ and $\Delta_{\mathrm{fus}}U_{\mathrm{m}}$ are reliable.

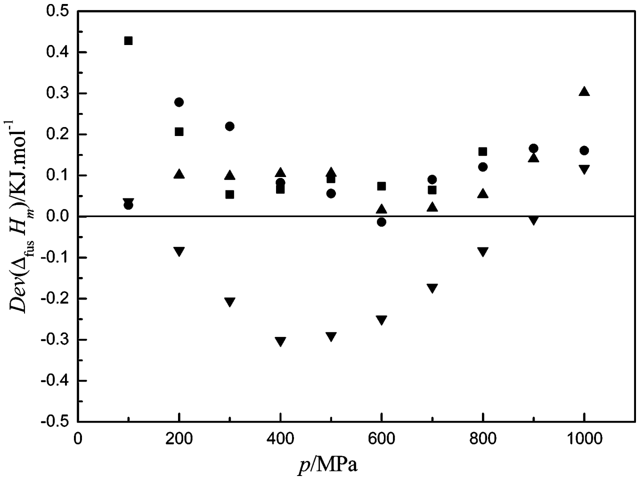

Figure 3. Deviations Dev($\Delta_{\mathrm{fus}}H_{\mathrm{m}}$) = $\Delta_{\mathrm{fus}}H_{\mathrm{m}}$(calcd) − $\Delta_{\mathrm{fus}}H_{\mathrm{m}}$(refs) of the calculated changes of molar enthalpy on fusion from those values from refs 3 and 4: ▼, benzene; ■, nitrobenzene; ●, bromobenzene; ▲, chlorobenzene.

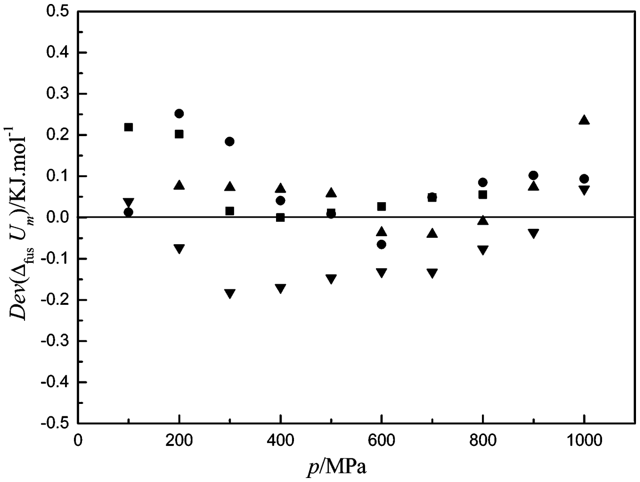

Figure 4. Deviations Dev($\Delta_{\mathrm{fus}}U_{\mathrm{m}}$) = $\Delta_{\mathrm{fus}}U_{\mathrm{m}}$(calcd) − $\Delta_{\mathrm{fus}}U_{\mathrm{m}}$(refs) of the calculated changes of molar internal energy on fusion from those values from refs 3 and 4: ▼, benzene; ■, nitrobenzene; ●, bromobenzene; ▲, chlorobenzene.

Conclusions

This paper describes a method of measuring the fusion temperatures at high pressures and reports on the fusion curves of benzene, nitrobenzene, bromobenzene, and chlorobenzene at pressures up to 3500 MPa. The fusion curves of four substances point conclusively to only one conclusion, namely, that the shapes of fusion curves are without maximum temperatures as Tammann had supposed. The fusion equations based on the two- and one-phase approaches were used to fit experimental data. Changes of the molar enthalpy and the molar internal energy on fusion were calculated using the parameters of a fitted equation. Comparisons with previously published results show that experimental and calculated data are reasonable.

Literature Cited

(1) Jeanloz, R. Physical chemistry at ultrahigh pressures and temperatures. *Annu. Rev. Phys. Chem.* **1989**, *40*, 237−259.

(2) Bridgman, B. W. Freezings and compressions to 50,000kg/cm^2. *Phys. Rev.* **1941**, *9*, 794−797.

(3) Bridgman, B. W. Change of phase under pressure. *Phys. Rev.* **1914**, *3*, 153−203.

(4) Bridgman, B. W. Change of phase under pressure. *Phys. Rev.* **1915**, *4*, 1−33.

(5) Osugi, J.; Shimizu, K.; Yasunami, K. Liquid−solid transition at high pressure III: benzene, monochlorobenzene and toluene at 25 °C. *Rev. Phys. Chem. Jpn.* **1968**, *38*, 90−95.

(6) Crawford, R.; Daniel, W. Experimental determination of $p-T$ melting curves of krypton, neon and helium. *J. Chem. Phys.* **1971**, *55*, 5651−5656.

(7) Strong, H. M.; Bundy, F. P. *The Use of Iron and Gold for Calibration of Higher Pressure and Temperature Points*; National Bureau of Standards: Washington, DC, 1971.

(8) Akella, J.; Kennedy, G. C. Melting point of gold, silver and copper—proposal for a new high pressure calibration scale. *J. Geophys. Rev.* **1971**, *76*, 4969−4977.

(9) Atkins, P.; Paula, J. D. *Atkins' Physical Chemistry*, 7th ed.; Oxford University Press: Oxford, U.K., 2002; pp 145−146.

(10) Kechin, V. V. Thermodynamically based melting-curve equation. *J. Phys.: Condens. Matter* **1995**, *7*, 531−535.

(11) Hausletner, C.; Hafner, J. A theoretical study of the melting curve of iron to very high pressure. *J. Phys.: Condens. Matter* **1989**, *1*, 5234−5252.

(12) Fried, L. E.; Howard, W. M. Explicit Gibbs free energy equation of state applied to the carbon phase diagram. *Phys. Rev. B* **2000**, *61*, 8734−8743.

(13) Babb, S. E. Parameters in the Simon equation relating pressure and melting temperature. *Rev. Mod. Phys.* **1963**, *35*, 400−413.

(14) Han, F.; Xue, Y.; Tian, Y. L. Vapor−liquid equilibria of the carbon dioxide + acetone system at pressures from (2.36 to 11.77) MPa and temperatures from (333.15 to 393.15) K. *J. Chem. Eng. Data* **2005**, *50*, 36−39.

(15) Jäger, J.; Wanninger, W. Strain gauge dilating-cylinder transducer for pressures up to 14 kbar. *Feinwerke−Technik.* **1976**, *84*, 387−391.

(16) Tammann, G. *Kristallisieren und Schmelzen*; Johann Ambrosius Barth: Leipzig, Germany, 1903.

(17) Dwight, E. G. *American Institute of Physics Handbook*, 3rd ed.; McGraw-Hill Book: New York, 1957.

Received for review May 21, 2007. Accepted July 2, 2007. T.Y. is grateful for a fellowship from the Internationales Seminar in Chemie-Ingenierwesen, Technischer und Physikalischer Chemie. We are thankful for financial support from a project of the National Natural Science Foundation of China (No. 20476071).

JE700276Z